Sub-Sahara African Academic Research Publications
September, 2021, Editions

JPAS
Journal of Pure and Applied Science
Vol..21, No.9, ISSN 2318-9315

OXIDATIVE STRESS MARKERS' PROFILES IN MCF-7 (BREAST CANCER) CELL-LINE TREATED WITH DOXORUBICIN LOADED ARAGONITE-CALCIUM CARBONATE NANOPARTICLES

***HAMIDU AHMED & **ZUKI ABU BAKAR**
**Laboratory Molecular Biomedicine, Institute of Bioscience, Universiti Putra Malaysia 43400 Serdang, Selangor Malaysia [Department of Biomedical and Pharmaceutical Technology, Federal Polytechnic Mubi]. **Department of Preclinical Science, Faculty of Veterinary Medicine, Universiti Putra Malaysia, Selangor 434000 Serdang, Selangor, Malaysia.*

Abstract:
This study was undertaken to investigate the mode of interaction of Doxorubicin Loaded Aragonite Calcium Carbonate Nanoparticles with tumoral MCF-7 cell lines, in order to understand the effect of these agents on cell organic molecules. Cockle shells, Acridine Orange, Propidium iodine Fetal bovine serum, tetrazolium bromide dye, antibiotics combination, Phosphate buffered saline, Doxorubicin hydrochloride, intracellular Reactive Oxygen Species Assay kit Superoxide dismutase, Hydrogen peroxide assay kit, Total Glutathione and Catalase activity assay kit were all used in the study. The results of the investigation indicate that treatment of MCF-7 cells with DOX-Ar-CC-NPs and DOX exhibited a dose-dependent effect on cell viability. The ability of DOX-NPs to induce apoptosis in MCF-7 cells was confirmed; indicting the high potency of Aragonite Calcium Carbonate Nanoparticles in drug delivery.

Keywords: *Oxidative stress; Doxorubicin; Nanoparticle; aragonite-calcium carbonate**;** Breast cancer; Cockle shell.*

Introduction

Decades of research in science and engineering has led to the development of precise molecularly structures and gadgets in the nanometre scales, and this

usually is popularly referred to as nanotechnology [1]. The nanomaterial at a nanoscale demonstrates new and distinctive properties which has facilitated its applications in medicine and life sciences [2]. This advancement has made nanomaterials pretty for utilisation for different items which has resulted in the development in the field of nanotechnology, because of the advantage guaranteed by the synthesis of nanomaterials into products [3]. Through the advancement of nanotechnology, the size impacts of particles have steadily been thought to be imperative [2]. Consequently, an enhanced potential threat, including exposure and risk evaluations, related to the introduction to nanomaterials is crucial to check its safety or toxicity [4]. Indeed, even though nanomaterials are as of now being generally utilised as a part of present-day innovation, there is a genuine absence of data concerning the human health and ecological effects of prepared nanomaterials [5].

The fundamental component of these nanomaterials is that in comparison with mass materials, calcium carbonate nanoparticles ($CaCO_3$ nanoparticles) have a higher surface area to volume proportion and therefore an upgraded contact region with their surroundings than do mass materials for drug delivery [6,7]. This could imply that synergist or other dynamic sites on the molecular surface are showing, at times initiating the arrangements of reactive oxygen species (ROS) [8]. Consequently, $CaCO_3$ nanoparticles are encapsulated in numerous cells and organs to a more considerable degree than are macro size particles [9]. A few $CaCO_3$ nanoparticles promptly delivered all through the body, accumulate in target organs, penetrate cell films, held up in mitochondria and may eventually trigger harmful reactions [10]. However, in comparison with unstructured mass material, the size, shape of cockle shell-derived $CaCO_3$ nanoparticles (Ar-CC-NPs) can assume a significant part in a determining reaction [11]. However, Ar-CC-NPs is notable for its anticancer action when used as a drug delivery carrier [12]. The primary aim of the present work was to study how Ar-CC-NPs interact with tumoral MCF-7 cell lines to understand the effect of such nanomaterial on organic cell molecules. In this study, we designed a nano anticancer-oxidative stress markers formulation using Doxorubicin loaded Cockle-shell Aragonite nanoparticles DOX-Ar-CC-NPs, a hydrophilic anticancer drug. Our primary goal was to evaluate the oxidative stress markers by MCF-7 cell line following treatment. The designed Ar-CC-

NPs-anticancer formulation was further evaluated for therapeutic efficacy against MCF-7 (Breast cancer) cells in vitro.

Materials and Methods

Synthesis, physicochemical characterisation and biocompatibility of Ar-CC-NPs and DOX-Ar-CC-NPs on MCF-7 Breast cancer cell-line
Details on these aspects have been earlier published [13].

Evaluation of changes in oxidative stress markers

Following treatment of the cells, they were assayed for the changes in oxidative stress markers using commercial ELISA OxiSelect assay Kit (Cell Biolabs, USA) according to the manufacturer's instruction. Enzymes assayed which comprises of Reactive Oxygen Species (Green Fluorescence), Superoxide Dismutase (SOD) Activity, Total Glutathione peroxide (GSSG/GSH), (Colorimetric) and Hydrogen Peroxide Assay.

Reactive oxygen species (ROS) assay

Intracellular reactive oxygen species (ROS) generation after the treatment of aragonite calcium carbonate nanoparticles (Ar-CC-NPs) was evaluated using 2,7–dichlorofluorescin diacetate (DCFH-DA) as described by the protocol and by Abdelaziz *et al.* (2018), Ahamed *et al.* (2016) and Rajabnia *et al.* (2018) with slight modification. Two techniques measured the ROS level; fluorometric quantitative assay and cell imaging. In preference to fluorometric quantitative assay, 1 x 10^5 cells/well were seeded in black cell culture fluorometric plates and allowed to attach on the surface for 24 hrs in a CO_2 incubator at 37^0C. Furthermore, after cells were treated with different concentrations (5, 25, and 100 g/mL) of DOX, DOX-Ar-CC-NPs, Ar-CC-NPs and Control for 24 hrs. After the exposure was completed, cells were washed with the media to each well twice-trice with DPBS before being incubated in 1 mL of working solutions of DCFH-DA for 30 min at 37^0C. Thereafter, cells were lysed in alkaline solution and centrifuged at 1500 g for 10 min. A 100 µL supernatant was transferred to a new suitable for fluorescence measurement at 480 nm excitation and 530 nm emissions utilising the microplate reader (Synergy-HT, BioTek, USA). The values were presented as a per cent of fluorescence intensity relative to control. A parallel set of cells (1 x 10^5 cells/well) in a 96-well plate

suitable for fluorescence were analysed for intracellular fluorescence using a fluorescence microscope (OLYMPUS CKX 41), with images taken at 200 x magnification.

Superoxide dismutase (SOD) activity

Superoxide dismutase activity was measured using a commercial colorimetric assay kit, OxiSelect SOD Activity (Cell Biolabs, Inc., San Diego, CA). In brief, MCF-7 cells were treated 24 hrs with MTT IC_{50} of the corresponding DOX, DOX-Ar-CC-NPs, Ar-CC-NPs and control for 72 hrs. After treatment, cells were rinsed with ice-cold PBS and then were incubated on ice with 1 x Lysis Buffer (10 mM Tris, pH 7.5, 150 mM NaCl, 0.1mM EDTA, 0.5 % Triton x -100) for 10 minutes. Later, cells were centrifuged at 12000 g for 10 minutes, and the cell lysate supernatant was collected and added (10 µl) to 96-well plate and then the main mixture was added. Finally, 10 µL 1 x Xanthine Oxidase Solution was added and immediately the absorbance was read at 490 nm.
The results were expressed as a percentage of SOD activity and were calculated as follows: SOD activity = $(A_0 – A_1)/A_0$I x 100, where A_0 is the absorbance of the negative control and A_1 is the absorbance of the cells exposed to the DOX, DOX-Ar-CC-NPs, Ar-CC-NPs and control.

Glutathione assay

The total Glutathione (GSH) level was determined using a commercial colorimetric assay kit, OxiSelect. Total glutathione (GSSG/GSH); Cell Biolabs, Inc.; San Diego, CA). In brief, the assay was evaluated according to the manufacturer's instructions. Concisely, DOX, DOX-Ar-CC-NPs, Ar-CC-NPs and Control were treated with 24 hrs IC_{50} of the corresponding DOX, DOX-Ar-CC-NPs, Ar-CC-NPs and Control for 24, 48, and 72 hrs. After treatment, cell was centrifuged and washed with cold 1 x PBS. The pellet was resuspended with 200-500 µL ice-cold 0.5% metaphosphoric acid (MPA), the cells were again centrifuged at 1200 rpm for 5 min at 4^0C, and the supernatant was collected. Then and there, 25 µL 1 x NADPH were added in 96-well plate and after that 100 µL of the samples were added. In conclusion, 50 µL x chromogen was added and mixed briefly. Immediately, the absorbance was recorded at 405 nm at 2 min intervals for 10 min. The total glutathione level was measured by comparison with the predetermined glutathione standard curve. The results

were expressed as a percentage of total glutathione (GSSG/GSH). Principle of this assay measures glutathione peroxidase activity indirectly by a coupled reaction with glutathione reductase. Oxidised glutathione, produced upon reduction of hydroperoxide by glutathione peroxidase, is recycled to its reduced state by glutathione reductase and NADPH:

$$R\text{-}O\text{-}O\text{-}H + 2GSH \xrightarrow{Glutathione\ Pexoxidase} R\text{-}O\text{-}H + GSSG + H_2O$$

$$GSSG + NADPH + H^+ \xrightarrow{Glutathione\ reductase} 2GSH + NADP^+$$

The oxidation of NADPH to $NADP^+$ is supplemented by a decrease in absorbance at 340 nm [16].

Hydrogen peroxide assay

Hydrogen peroxide assay was determined according to the product manual Oxiselect^{TM} Hydrogen peroxide assay kit (Colorimetric) catalogue number STA.844 (CELL BIOLABS, INC USA). Four wells were designated as DOX, DOX-Ar-CC-NPs, Ar-CC-NPs and Control. To each well, 50 µL of each sample was assayed in triplicate (H_2O_2 standard and control) into an individual microliter plate well. To standard well, 50 µL of hydrogen peroxide working solution was added to each well. The contents were mix thoroughly and incubated for 30 minutes at room temperature protected from light. The decrease in the absorbance was read with a microplate reader in the 540 - 570 nm range using TECAN (RT 2100C) plate reader.

Cell cycle assay

Cell cycle assay was evaluated using cycle-test Plus DNA reagent kit (BD Bioscience, USA). In briefly, MCF-7 cells were seeded at 5 x 10^5 cells per well in six-well plates and incubated for 24 hrs, with equivalent concentration DOX alone for 24, 48 and 72 hrs. The cells were then treated with the IC_{50} of DOX, DOX-Ar-CC-NPs, Ar-CC-NPs (0.5 µg/mL) and control. The complete growth medium (Untreated Cells) served as the control. After each treatment, the adherent and floating cells were collected, and the seeded cells were suspended with 250 µL of trypsin buffer. After 5 minutes, 200 µL of trypsin inhibitor with 50 µL RNase a buffer was added. Finally, the samples cell was stained with 500 µL Propidium Iodide (PI) solution and incubated on ice for 30 minutes. The samples cells were run on a flow cytometer (Becton Dickinson, USA).

Statistical analysis

All statistical analysis was done using SPSS software (IBM SPSS Statistics version 23, USA) Comparisons between groups were determined using one-way analysis of variance (ANOVA), followed by post hoc group comparison of Dennett's multiple range test, significance was attributed at $p<0.05$ unless indicated otherwise. All experiments were conducted at least three times.

Results

Reactive oxygen species assay

Quantitative data suggested that DOX-Ar-CC-NPs induced ROS generation in a dose-dependent manner ($p<0.05$) (Figure 1-2). Similarly, fluorescent microscopy data also showed that DOX-Ar-CC-NPs treated cells and DOX alone express a high intensity of green fluoresce DCF dye as compared to the Control and Ar-CC-NPs (Figure 1-2). Despite this, increase in fluorescence intensity at higher concentrations is an indicator that DOX may generate more ROS as the concentration and time increases, which in due course results in cell damage.

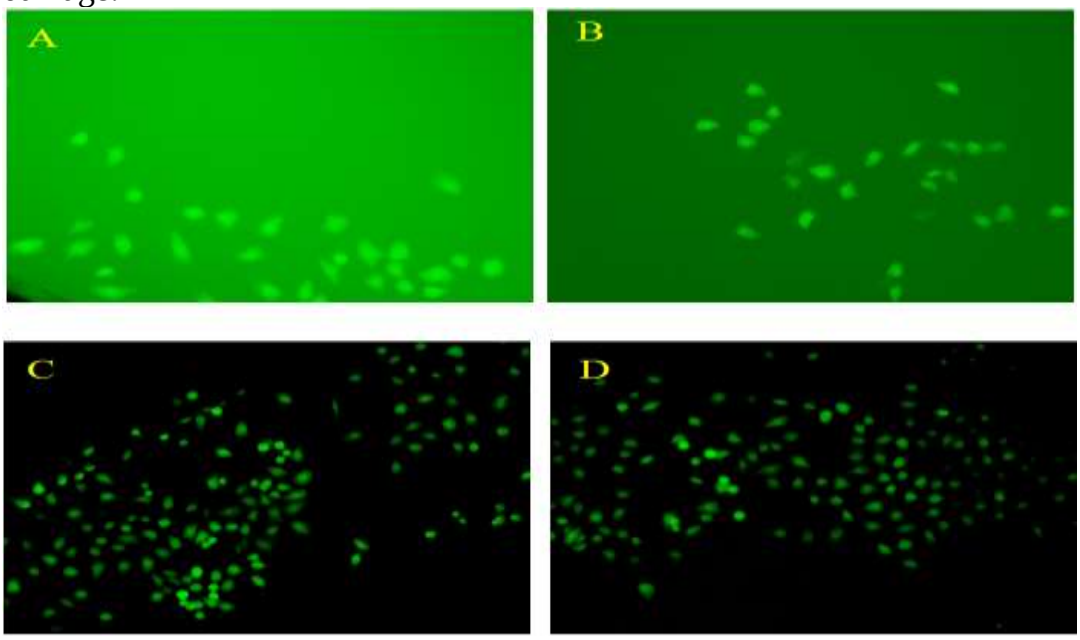

Figure 1: DOX-Ar-CC-NPs induced oxidative stress on MCF-7 cells exposed to DOX-Ar-CC-NPs, DOX alone and Ar-CC-NPs at IC_{50} dosages 0.5 mg/ml for 72 hrs. Show A) Fluorescence microscopy images of ROS generation, B) Shows Hydrogen peroxide level, C) Shows Cells treated with DOX-Ar-CC-NPs, D) Shows DOX alone with a high intensity of green fluorescent DCF dye.

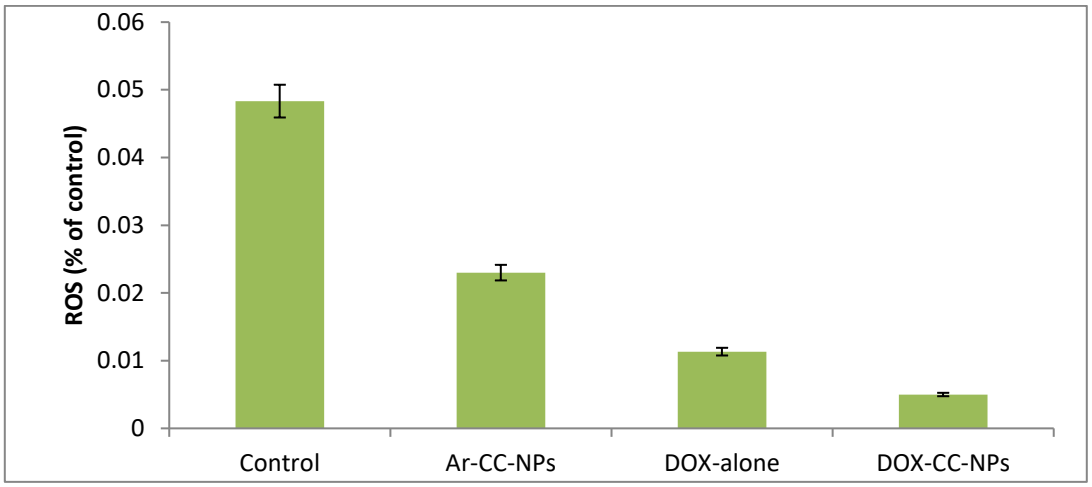

Figure 2: Data represented are mean ± SD of three identical experiments made in three replicate. There is a significant difference as compared to control (p<0.05), Ar-CC-NPs, DOX-Alone, and DOX Ar-CCPs

Glutathione assay

The enzymes assayed for total Glutathione peroxide was done throughout the study is shown in Figure 3. The non-significant different of total glutathione assay was observed in the DOX alone, DOX-Ar-CC-NPs, Ar-CC-NPs and control (p=0.3783). The glutathione assay (GSSH/GSH) was significantly increased (p= 0.0467) as compared to Ar-CC-NPs. However, there was also significantly differences observed in the DOX alone and control as compared to the other groups (p=0.0467). Also, there was also non-significant different in the DOX-Ar-CC-NPs and Ar-CC-NPs (P=0.4598) as compared to the other groups. Also, there were no significant changes between DOX-Ar-CC-NPs and control (p=45983). Besides, no significant difference was recorded between Ar-CC-NPs and control group as compared to others (p=0.9999).

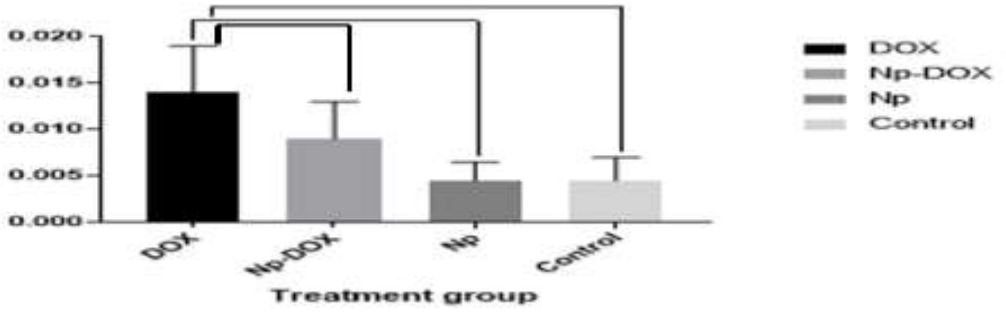

Figure 3: Evaluations of changes in oxidative stress markers for MCF-7 cells show the treatment groups with DOX, DOX-Ar-CC-NPs, Ar-CC-NPs and control for 72 hrs. Values are expressed as mean standard deviation. Different treatments indicate statistical significance (p< 0.05) between groups at different treatment

Hydrogen per oxide

DOX and DOX-Ar-CC-NPs induced oxidative stress. We investigated the ability of DOX alone and DOX-Ar-CC-NPs to cause oxidative stress by altering intracellular redox status (Figure 4-5). Intracellular ROS production was measured via the production of 2, 7-dichlorofluorescein (DCF) using a fluorescence assay. Quantitative data suggested that Dox-Ar-CC-NPs induced ROS generation in a dose-dependent manner ($p<0.05$). Similarly, fluorescent microscopy data also showed that DOX and Dox-Ar-CC-NPs treated cells express a high intensity of green fluoresce (DCF dye) as compared to control. Furthermore, the antioxidant GSH level was significantly lower in a dose-dependent manner in breast cancer cells (MCF-7 cells) exposed to DOX-Ar-CC-NPs.

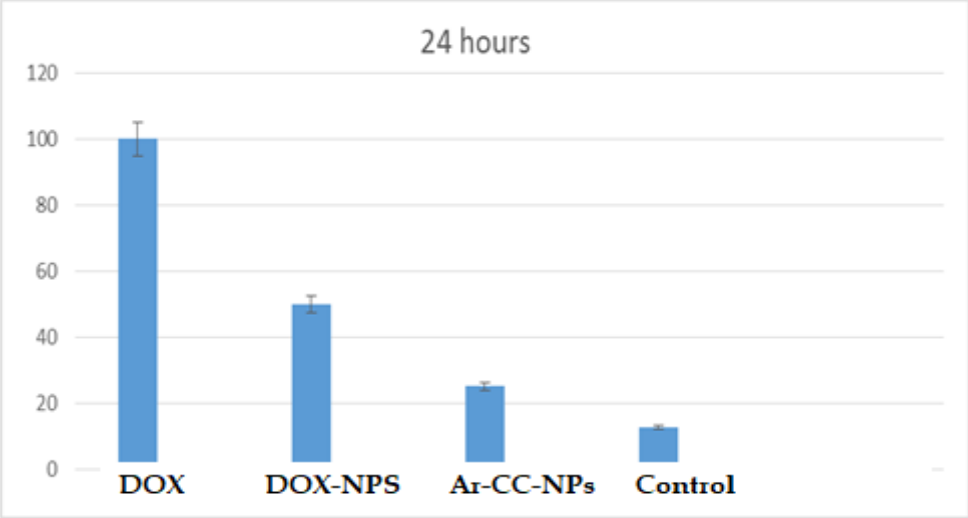

Figure 4: Hydrogen Peroxide Activity for MCF-7 cells show the treatment groups with DOX, DOX-Ar-CC-NPs, Ar-CC-NPs and control groups for 24 hrs. Values are expressed as mean standard deviation. Different

treatments indicate statistical significance (p< 0.05) between groups at different treatment

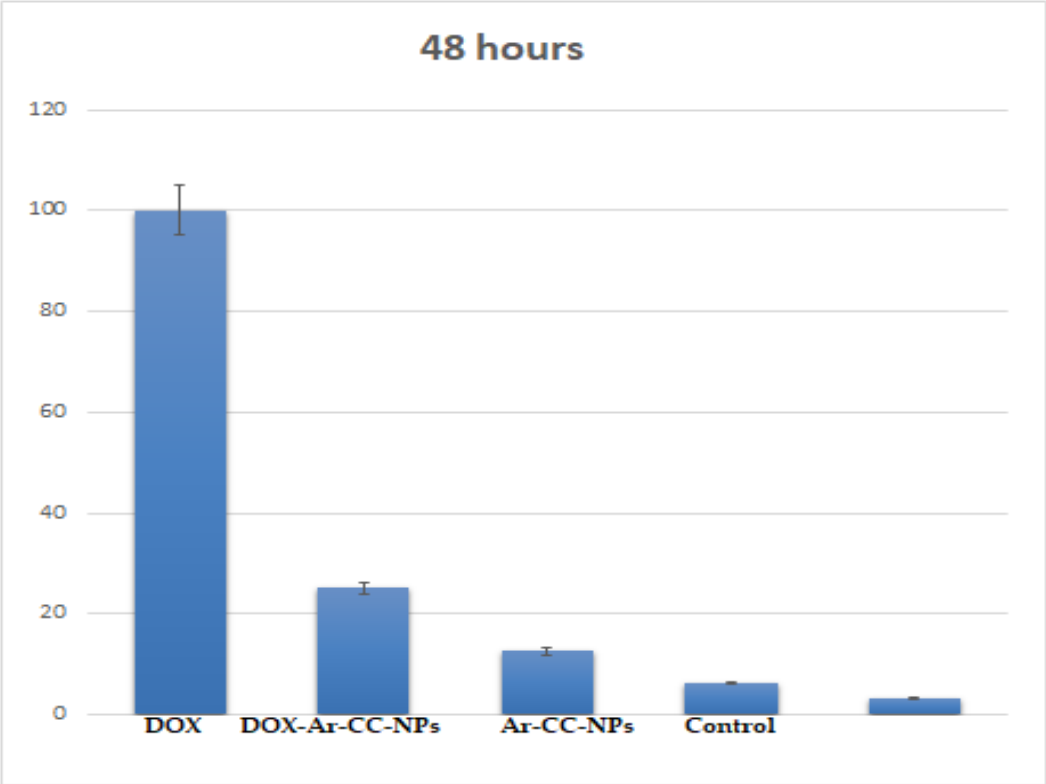

Figure 0: Hydrogen Peroxide Activity for MCF-7 treatment groups with DOX, DOX-Ar-CC-NPs, Ar-CC-NPs and control for 48 hrs Values are expressed as mean standard deviation. Different treatments indicate statistical significance (p< 0.05) between groups at different treatment

Cell cycle assay by DOX and DOX-Ar-CC-NPs

As demonstrated on DNA content, cell cycle analysis arrest consists of four phases: normal DNA content, 2N, (G2), DNA synthesis (S), double DNA content, 4N G2/G1 (G2/M) (Fu et al., 2017; Gérard et al., 2014). The apoptotic cells inhibit fractional DNA substances, stated as sub G2 (G0/G1). Any interruption in cell cycle assay regression may finally lead to apoptotic cell death (Wan et al., 2016). To ascertain the distribution of the MCF-7 cells in different phases of the cell cycle analysis, DNA content in the cells was

observed by propidium Iodide staining and flow cytometry for 24, 48 and 72 hrs. The flow cytometry histograms of MCF-7 cells treated with Ar-CC-NPs, DOX alone, and DOX-Ar-CC-NPs are presented below (Figure 6-I; 6-II; 6-III).

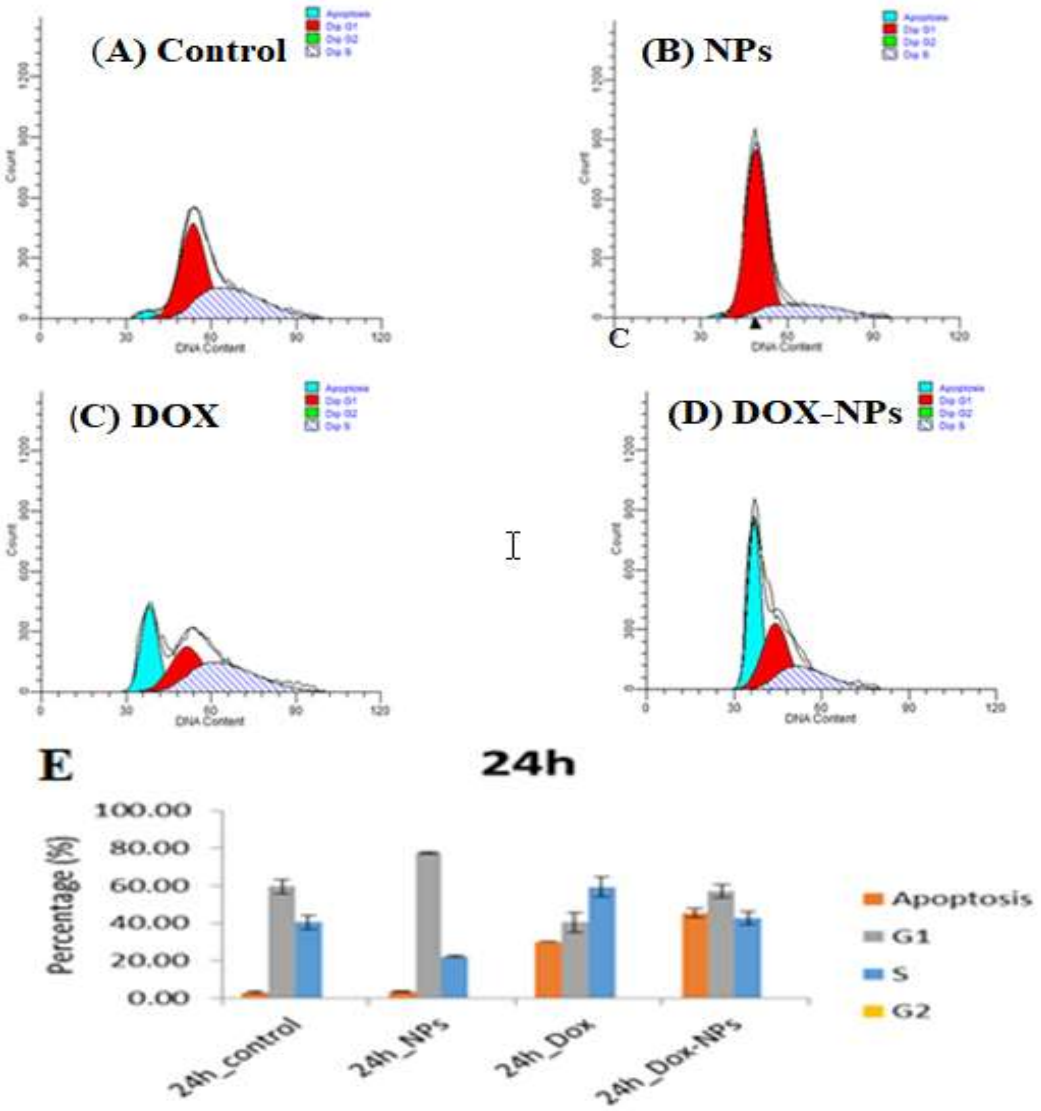

Figure 6-I: Cell cycle analyses of MCF-7 cells for 24 hrs. in different show A) Control group, B) Ar-CC-NPs treatment group, C) DOX treatment group, D) DOX-Ar-CC-NPs treatment group, and E) the quantification of cell cycle phase distributions of MCF-7 cells in different groups. Note: DOX-Ar-CC-NPs treatment group killed more cells (refer to percentage of apoptosis) as compared to DOX, with similar trend at 24 hrs p>0.05 compared with the control group

Table 1: Effect of DOX, DOX-Ar-CC-NPs and Ar-CC-NPs treatments on the breast cancer (MCF-7 cells) cell cycle for 24, 48 and 72 hrs in different groups

Time	Groups	G1	G2	G2/G1	S
24 hrs.	Control	56.92 ± 53.59%	0.00 ±79.33%	1.48 ± 0.1%	43.08±0.00%
	Ar-CC-NPs	78.00±50.81%$^{\Phi}$	0.00 ±79.88%$^{\Phi}$	1.57± 0.00%$^{\Phi}$	22.00± 0.00%$^{\Phi}$
	DOX	44.18± 51.56%$^{\Phi\Phi}$	0.04± 75.18%$^{\Phi\Phi}$	1.46±0.00%$^{\Phi\Phi}$	55.78%±0.00%$^{\Phi\Phi}$
	DOX-Ar-CC-NPs	54.79±44.48%$^{\Phi\Phi\Phi}$	0.04±55.66%$^{\Phi\Phi\Phi}$	1.25±0.00%$^{\Phi\Phi\Phi}$	45.18±0.00%$^{\Phi\Phi\Phi}$
48 hrs.	Control	81.02±50.39%	0.00±73.59%	1.46±0.00%	18.98±0.00%
	Ar-CC-NPs	78.89±49.22%$^{\Phi}$	0.00±81.27%$^{\Phi}$	1.65±0.00%$^{\Phi}$	21.11±0.00%$^{\Phi}$
	DOX	30.86±54.58%$^{\Phi\Phi}$	0.28±80.04%$^{\Phi\Phi}$	1.47±0.00%$^{\Phi\Phi}$	68.88±0.00%$^{\Phi\Phi}$
	DOX-Ar-CC-NPs	66.55±50.16%$^{\Phi\Phi\Phi}$	0.00±62.98%$^{\Phi\Phi\Phi}$	1.26±0.00%$^{\Phi\Phi\Phi}$	33.45±0.00%$^{\Phi\Phi\Phi}$
72 hrs.	Control	93.12±4573%	0.00±78.65%	1.72±0.00%	6.86±0.00%
	Ar-CC-NPs	93.4±45.07%$^{\Phi}$	0.00±62.46%$^{\Phi}$	1.39±0.00%$^{\Phi}$	1.39±0.00%$^{\Phi}$
	DOX	28.74±52.17%$^{\Phi\Phi}$	0.00±78.94%$^{\Phi\Phi}$	1.72±0.00%$^{\Phi\Phi}$	6.86±0.00%$^{\Phi\Phi}$
	DOX-Ar-CC-NPs	53.78±46.27%$^{\Phi\Phi\Phi}$	0.00±78.16%$^{\Phi\Phi\Phi}$	1.65±0.00%$^{\Phi\Phi\Phi}$	46.22±0.00%$^{\Phi\Phi\Phi}$

Note: $^{\Phi}$ $p>0.05$, $^{\Phi\Phi}$ $p<0.05$ and $^{\Phi\Phi\Phi}$ $p<0.01$ compared with the control untreated group.

Table 1 exhibits the effect of Ar-CC-NPs, DOX-alone and DOX-Ar-CC-NPs on percentage of MCF-7 cells extant in each cell cycle phase (G1, G2, S and G2/M). The untreated cells in control group were incubated for 24 hrs and observed to present a normal predominant distribution in G1 phase (0.00 ±79.33%), however a comparatively minor G2/M (1.48 ± 0.1%) and G1 (56.92 ± 53.59%) were observed. Furthermore, after the 24 hrs, the incubated cells with Ar-CC-NPs alone, yield a cell population in the G2 phase of 0.00 ±79.88%, while in G2/G1 phase it was 1.57± 0.00% and in G1 phase was 78.00±50.81%. There was no significant difference between Ar-CC-NPs alone treated group and control group in G1 and G2/G1 phases (P>0.05). As shown in Figure 5.8, 5.9, 5.10, the G2/G1 phase population increased from 1.48 ± 0.1% (control group) to 44.18± 51.56% while an increased quantity of cell population in G1 (54.79±44.48%) can as well be observed in DOX-Ar-CC-NPs treated group, which signified cell cycle arrest in G1 in these two treatment groups. The increased of cell population at the G1 phase was to be associated with a decreased of cell population G2 (0.04±55.66%) of the cell cycle treated group (DOX-Ar-CC-NPs). As well, the cell population in G1 phase was also

decreased at 48 hrs from 30.86±54.58% (DOX group) to 66.55±50.16% (DOX-Ar-CC-NPs group) and at 72 hrs, decreased from 28.74±52.17% (DOX group) to 53.78±46.27% (DOX-Ar-CC-NPs group). Cells treated with DOX-alone and DOX-Ar-CC-NPs showed a higher significant increase of the G2/G1 phase and G2 phase, compared with the control untreated group ($p<0.01$). These results demonstrated that DOX-Ar-CC-NPs induced cell cycle arrest in the G2/G1 phase and apoptosis in MCF-7 cells. Furthermore, these results signified the induction of cell cycle arrest and apoptosis of DOX-Ar-CC-NPs existed in a time-dependent manner and cause cycle arrest in the G1/G2 phase, and finally cell dearth through apoptosis.

Discussion

Further to the earlier detailed documentation on the synthesis, physicochemical characterisation and biocompatibility of Ar-CC-NPs and DOX-Ar-CC-NPs [13], this present study explored the ability of DOX and DOX-Ar-CC-NPs to induce cytotoxicity by altering the intracellular oxidative condition in ROS production. The generation of ROS by DOX is generally considered as a significant contributor to DOX toxicity and their formation, by exceeding the cellular defensive capability and causing oxidative damage to biomolecules [17,18]. ROS can also affect cell function by directly acting on cell components, including lipids, protein, and DNA, by destroying their structure, ultimately leading to cell death. In this study, the intracellular ROS generation was estimated through the production of 2, 7-dichlorofluorescein (DCF) using a fluorescence assay. Oxidative stress can also be expressed in terms of intracellular GSH level. GSH is an essential antioxidant that is oxidised during oxidative stress [19]. Our findings demonstrated DOX and DOX-Ar-CC-NPs induced ROS generation, GSH and Hydrogen peroxide depletion in MCF-7 cells. Besides, cytotoxicity of DOX was effectively abrogated by an antioxidant ROS scavenger. These results suggested that ROS could be one of the critical pathways of toxicity caused by DOX to MCF-7 cells. Some recent findings have implicated the production of ROS in the cytotoxicity mediated by spinel ferrite NPs [1,20].

Additionally the overall ROS assay outcomes of the Ar-CC-NPs on MCF-7 provide useful understanding into oxygen metabolism where ROS signify to radicals or chemical and molecules that comprise of ROS compounds such as

peroxides resulting from normal oxygen metabolic rate with vital roles in cell and homeostasis signalling [21,22]. This study was intended to normalise population units of the cells lines in which the results in this study (Figure.5.5) revealed that the DOX-Ar-CC-NPs treated MCF-7 cells exhibited higher reactive oxygen species as compared to the DOX alone treated cells. Reactive oxygen species generation of the DOX was significantly lower than on DOX-Ar-CC-NPs and demonstrated consistent ROS generation also in agreement with previous biocompatibility results further highlighting the remarkability of DOX-Ar-CC-NPs. For that reason, these results could be elucidated by the fact that the internalisation of Ar-CC-NPs possibly induced oxidative stress which in turn triggered cell death demonstrated in the results. For this study support evidences that induction of environmental stress drastically increases reactive oxygen species levels triggering substantial cellular damage also identified as oxidative stress [22,23]. In addition, it also, validates the findings of previous works in which cancer cells generate high levels of ROS. Increased metabolic rate activities of peroxisomes in addition also explain this, oxidase and cellular dysfunction and mitochondria [24,25].

Consistent with earlier literature, this study also found works that stated NPs cellular uptake to induce mitochondrial membrane permeability and disrupting the respiratory chain causing apoptosis. In the same way it has been discussed that for local cancer therapy that Burkitt lymphoma B cells and epithelial breast cancer cells caused possible damage using targeted irradiation and gold-NPs causing high reactive oxygen species generation leading to cellular apoptosis and necrosis but while sustaining minimal damage to adjacent particle-free tissue [26]. Additionally, it has been established that carbon and metallic nanomaterial generate minimal ROS however aggregation, size, the morphology, cellular interaction and nano-metallic ions influence oxidative stress release causing physiological dysfunction of the cell which in turn prompts DNA damage [26,27]

Conclusion

Treatment of MCF-7 cells with DOX alone and DOX-Ar-CC-NPs exhibited a dose-dependent validity on cell viability. The DOX-Ar-CC-NPs had a significant inhibitory effect on cell viability compared to DOX alone ($p<0.05$). A similar trend was noticed in oxidative stress markers. Besides, the results

clearly showed that DOX-Ar-CC-NPs induced ROS generation of MCF-7 cells. However, treatment with DOX-Ar-CC-NPs significantly decreased the elevated level of superoxide dismutase 2 (SOD 2) compared to the untreated MCF-7 cells (control group). Hydrogen peroxide significantly increased the formation of ROS by DOX-Ar-CC-NPs compared to the untreated control. Furthermore, Glutathione assay revealed apoptosis bodies on DOX-Ar-CC-NPs treated cells. Thus, it implies that DOX-Ar-CC-NPs induced apoptosis in breast cancer cells. DOX and DOX-Ar-CC-NPs were similarly established to induce oxidative stress evident by ROS generation, GSH and Hydrogen peroxide depletion. Cytotoxicity caused by DOX as effectively abrogated by ROS scavenger signifying that oxidative stress could be one of the mechanisms of cytotoxicity of this DOX. Additional investigations are underway to explore the cytotoxicity mechanism of DOX within different types of human cancer cells and *in vivo* using an animal model. Finally, our findings revealed the ability of DOX-Ar-CC-NPs to induce apoptosis in MCF-7 cells, which indicates high potency of the Ar-CC-NPs for anticancer drug delivery.

Author Contributions: "Conceptualization, H.A.; and M.Z.A.B.; Methodology, H.A.; M.A.; R.M.; and I.S.A.R.; Validation, H.A.; M.Z.A.B.; and J.R.A.; Formal analysis, H.A.; M.Z.A.B.; and J.R.A; Investigation, H.A.; B.G.; and A.D.; X.X.; Writing—original draft preparation, H.A.; M.Z.A.B.; B.G.; and A.D.; Writing—review and editing, All authors.; Supervision, M.Z.A.B.; M.A; R.M.; and I.S.A.R.; Project administration, M.Z.A.B.; Funding acquisition, M.Z.A.B.; All authors have read and agreed to the published version of the manuscript.

Funding: This research was funded by Universiti Putra Grant (IPS/9578300) and the Fundamental Research Grant Scheme (FRGS/5540031).

Acknowledgments: The authors wish to acknowledge the support of the staffs of Microscopy laboratory unit, Institute of Bioscience and the Biochemistry unit, Universiti Putra Malaysia, for their assistance during the analysis.

Conflicts of Interest: The authors declare no conflict of interest.

References

1. Ahamed, M.; Akhtar, M.J.; Alhadlaq, H.A.; Khan, M.A.M.; Alrokayan, S.A. Comparative cytotoxic response of nickel ferrite nanoparticles in human liver HepG2 and breast MFC-7 cancer cells. *Chemosphere* **2015**, *135*, 278–288,

doi:10.1016/j.chemosphere.2015.03.079.
2. Dudefoi, W.; Villares, A.; Peyron, S.; Moreau, C.; Ropers, M.; Gontard, N.; Cathala, B. Nanoscience and nanotechnologies for biobased materials , packaging and food applications : New opportunities and concerns. *Innov. Food Sci. Emerg. Technol.* **2018**, *46*, 107–121, doi:10.1016/j.ifset.2017.09.007.
3. Colombo, S.; Beck-broichsitter, M.; Peter, J.; Malmsten, M.; Rantanen, J.; Bohr, A. Transforming nanomedicine manufacturing toward Quality by Design and micro fl uidics ☆. *Adv. Drug Deliv. Rev.* **2018**, *128*, 115–131, doi:10.1016/j.addr.2018.04.004.
4. Liu, M.; Zheng, S.; Zhang, X.; Guo, H. Cerenkov luminescence imaging on evaluation of early response to chemotherapy of drug-resistant gastric cancer. *Nanomedicine Nanotechnology, Biol. Med.* **2018**, *14*, 205–213, doi:10.1016/j.nano.2017.10.001.
5. Elena, A.; Vidal, V.; Carrière, M.; Hiram, A.; Levard, C.; Chaurand, P.; Sarret, G.; Elena, A.; Vidal, V.; Carrière, M.; et al. Silver nanoparticles and wheat roots : a complex interplay To cite this version : HAL Id : hal-01516961. **2018**.
6. Render, D.; Samuel, T.; King, H.; Vig, M.; Jeelani, S.; Babu, R.J.; Rangari, V. Biomaterial-Derived Calcium Carbonate Nanoparticles for Enteric Drug Delivery. **2016**, *2016*.
7. Patra, J.K.; Das, G.; Fraceto, L.F.; Vangelie, E.; Campos, R.; Rodriguez, P.; Susana, L.; Torres, A.; Armando, L.; Torres, D.; et al. Nano based drug delivery systems : recent developments and future prospects. *J. Nanobiotechnology* **2018**, 1–33, doi:10.1186/s12951-018-0392-8.
8. Rajabnia, T.; Meshkini, A. Fabrication of adenosine 5 ′ -triphosphate-capped silver nanoparticles : Enhanced cytotoxicity e ffi cacy and targeting e ff ect against tumor cells. **2018**, *65*, 186–196, doi:10.1016/j.procbio.2017.11.003.
9. Weitz, D.A. Gold Nanorods Conjugated Porous Silicon Nanoparticles Encapsulated in Calcium Alginate Nano Hydrogels Using Microemulsion Templates. **2018**, doi:10.1021/acs.nanolett.7b05210.
10. Chen, D.; Weitz, D.A. Gold Nanorods Conjugated Porous Silicon Nanoparticles 2 Encapsulated in Calcium Alginate Nano Hydrogels Using 3 Microemulsion Templates 1. **2018**, doi:10.1021/acs.nanolett.7b05210.
11. Kamba, A.S.; Ismail, M.; Ibrahim, T.A.T.; Zakaria, Z.A.B. Research Article Synthesis and Characterisation of Calcium Carbonate Aragonite Nanocrystals from Cockle Shell Powder (Anadara granosa). *J. Nanomater.* **2013**, *2013*.
12. Hammadi, N.I.; Abba, Y.; Noor, M.; Hezmee, M.; Shameha, I.; Razak, A.; Jaji, A.Z.; Isa, T.; Mahmood, S.K.; Abu, Z.; et al. Formulation of a Sustained Release Docetaxel Loaded Cockle Shell-Derived Calcium Carbonate Nanoparticles against Breast Cancer. **2017**, 1193–1203, doi:10.1007/s11095-017-2135-1.
13. Hamidu, A.; Mokrish, A.; Mansor, R.; Shameha Abdul Razak, I.; Danmaigoro, A.; Zubair Jaji, A.; Abu Bakar, Z. Modified methods of nanoparticles synthesis in pH-sensitive nano-carriers production for doxorubicin delivery on MCF-7 breast cancer cell line. **2019**, doi:10.2147/IJN.S190830.
14. Ahamed, M.; Javed, M.; Alhadlaq, H.A.; Alshamsan, A. Colloids and Surfaces B : Biointerfaces Copper ferrite nanoparticle-induced cytotoxicity and oxidative stress in human breast cancer MCF-7 cells. *Colloids Surfaces B Biointerfaces* **2016**, *142*, 46–54, doi:10.1016/j.colsurfb.2016.02.043.
15. Abdelaziz, H.M.; Gaber, M.; Abd-elwakil, M.M.; Mabrouk, M.T.; Elgohary, M.M.; Kamel, N.M.; Kabary, D.M.; Freag, M.S.; Elzoghby, A.O. Inhalable particulate drug

delivery systems for lung cancer therapy : Nanoparticles , microparticles , nanocomposites and nanoaggregates. *J. Control. Release* **2018**, *269*, 374–392, doi:10.1016/j.jconrel.2017.11.036.
16. González De Vega, R.; García, M.; Fernández-Sánchez, M.L.; González-Iglesias, H.; Sanz-Medel, A. Protective effect of selenium supplementation following oxidative stress mediated by glucose on retinal pigment epithelium. *Metallomics* **2018**, *10*, 83–92, doi:10.1039/c7mt00209b.
17. Zhang, Y.; Ma, P.; Wang, Y.; Du, J.; Zhou, Q.; Zhu, Z.; Yang, X.; Yuan, J. Biocompatibility of Porous Spherical Calcium Carbonate Microparticles on Hela Cells. *World J. Nano Sci. Eng.* **2012**, *02*, 25–31, doi:10.4236/wjnse.2012.21005.
18. Saleha, A.A.; Khor, K.H.; Zunita, Z.; Jalila, A. Faculty of Veterinary Medicine, Universiti Putra Malaysia, UPM Serdang, Selangor, Malaysia. **2015**, *27*, 7–11.
19. Davies, K.J.A. Oxidative Stress , Antioxidant Defenses , and Damage Removal , Repair , and Replacement Systems. **2000**, 279–289.
20. Ahamed, M.; Akhtar, M.J.; Khan, M.A.M.; Alrokayan, S.A.; Alhadlaq, H.A. Oxidative stress mediated cytotoxicity and apoptosis response of bismuth oxide (Bi2O3) nanoparticles in human breast cancer (MCF-7) cells. *Chemosphere* **2019**, *216*, 823–831, doi:10.1016/j.chemosphere.2018.10.214.
21. Seabra, A.B.; Durán, N. Nanotoxicology of Metal Oxide Nanoparticles. **2015**, 934–975, doi:10.3390/met5020934.
22. Zhang, Y.; Gu, A.Z.; Xie, S.; Li, X.; Cen, T.; Li, D.; Chen, J. Nano-metal oxides induce antimicrobial resistance via radical-mediated mutagenesis. *Environ. Int.* **2018**, *121*, 1162–1171, doi:10.1016/j.envint.2018.10.030.
23. Anwar, A.; Gould, E.; Tinson, R.; Iqbal, J.; Hamilton, C. Redox Modulation at Work : Natural Phytoprotective Polysulfanes From Alliums Based on Redox-Active Sulfur. **2018**, 397–407.
24. Hong, S.M.; Hwang, S.W.; Wang, T.; Park, C.W.; Ji, J.J.; Kim, H.S.S.; Lee, J.L.; Kim, C.W.; Yoon, G.; Kim, K.H.; et al. Increased nicotinamide adenine dinucleotide pool promotes colon cancer progression by suppressing reactive oxygen species level. **2019**, 629–638, doi:10.1111/cas.13886.
25. Sgarbi, G.; Gorini, G.; Liuzzi, F.; Solaini, G.; Baracca, A. Hypoxia and IF 1 Expression Promote ROS Decrease in Cancer Cells. **2018**, 1–12, doi:10.3390/cells7070064.
26. Kiranda, H.K.; Mahmud, R.; Abubakar, D.; Zakaria, Z.A. Fabrication , Characterization and Cytotoxicity of Spherical-Shaped Conjugated Gold-Cockle Shell Derived Calcium Carbonate Nanoparticles for
27. Mao, B.; Chen, Z.; Wang, Y.; Yan, S. Silver nanoparticles have lethal and sublethal adverse effects on development and longevity by inducing ROS-mediated stress responses. *Sci. Rep.* **2018**, 1–16, doi:10.1038/s41598-018-20728-z.